

Article

TEOS-PDMS-Calcium Oxalate Hydrophobic Nanocomposite for Protection and Stone Consolidation

Pagona-Noni Maravelaki , Kali Kapetanaki  and Dimitrios Stefanakis

School of Architecture, Technical University of Crete, Akrotiri, 73100 Chania, Greece; kkapetanaki@isc.tuc.gr (K.K.); dstefanakis1@isc.tuc.gr (D.S.)

* Correspondence: pmaravelaki@isc.gr

Abstract: A treatment for both protection and consolidation, was synthesized in a simplified procedure through the sol gel process. Synthesized nano-calcium oxalate (CaOx) was incorporated into tetraethoxysilane (TEOS) and polydimethylsiloxane (PDMS), providing a hybrid hydrophobic consolidant nanocomposite. Oxalic acid was selected due to its ability to catalyse the hydrolysis of TEOS, as a drying control agent, but also because of its contribution at the formation of the calcium oxalate in reaction with calcium hydroxide. CaOx, incorporated into the silica matrix of the final copolymer, exhibits interfacial compatibility with the stone substrate and simultaneously strengthens the treated surface, since CaOx appears to be more stable than calcium carbonate. The hydrolysis of TEOS, as well as the formation of CaOx was evaluated through thermogravimetric analysis (TG/DTA). The nanocomposite consists of particles with approximately 7–700 nm in size range, as shown in TEM images. The consolidation, in combination with the hydrophobicity of surface resulted in an increase of the resistance to decay. Mechanical properties were enhanced as evaluated by ultrasonic pulse velocity on treated and untreated surfaces. Furthermore, water contact angle, as well as water absorption by capillarity test, showed improved water repellency of treated stones. Finally, this treatment doesn't alter the aesthetic surface parameters, a fact that is essential in cultural heritage conservation, while the consolidant remains intact under UV and moisture exposure.

Keywords: stone impregnation; hydrophobic nanocomposite; TEOS-calcium oxalate consolidant



Citation: Maravelaki, P.-N.; Kapetanaki, K.; Stefanakis, D. TEOS-PDMS-Calcium Oxalate Hydrophobic Nanocomposite for Protection and Stone Consolidation. *Heritage* **2021**, *4*, 4068–4075. <https://doi.org/10.3390/heritage4040224>

Academic Editor: Nicola Masini

Received: 12 October 2021

Accepted: 28 October 2021

Published: 30 October 2021

Publisher's Note: MDPI stays neutral with regard to jurisdictional claims in published maps and institutional affiliations.



Copyright: © 2021 by the authors. Licensee MDPI, Basel, Switzerland. This article is an open access article distributed under the terms and conditions of the Creative Commons Attribution (CC BY) license (<https://creativecommons.org/licenses/by/4.0/>).

1. Introduction

Cultural heritage buildings mostly consist of stone and lime-based mortars. These architectural surfaces are subjected to decay due to natural processes, as well as anthropogenic actions. Various nanocomposites have been widely investigated and used as protective agents over the last years.

Such products are based on a consolidant known as TEOS, which forms SiO₂ nanoparticles through a sol-gel process maintaining decohesion at grains of stone substrate [1–3]. However, TEOS based consolidants possess several disadvantages like cracking, insufficient bonding to carbonaceous substrates and hydrophilicity [4].

In order to preponderate these drawbacks, we designed a modified TEOS based consolidant nanocomposite; calcium oxalate (CaOx) has been integrated into silica matrix, in order to achieve chemical affinity with the carbonaceous nature of limestones. It is well-known that calcium oxalate has played a crucial, protective role in monuments, since quantity of it has been detected in the patina, present on historical surfaces that have been maintained in fairly good conditions [5,6].

Another innovation of this synthesis is the formation of calcium oxalate during the polymerization of TEOS, as well as the addition of a hydrophobic agent, PDMS (hydroxyl-terminated polydimethylsiloxane). PDMS is an organosilane, which provides hydrophobicity, water repellency and reduces the surface energy, eliminating in that way the formation of cracks. The hydrophobic chains of PDMS cause some gaps in the resulting network, contributing to increased deformability and porosity.

The aforementioned product was applied on porous limestones called “alfas” originating from a specific quarry of the island of Crete and are commonly used as building stones for monument reconstruction. This type of limestone is very porous, with massive texture, whereas its open porosity has been measured equal to 17.92% (± 1.58) [7]. The pore size distribution has been investigated by Verganelaki et al. and the total porosity was measured 32.7% [8].

2. Experimental Part

The synthetic procedure of the consolidant can be described in Figure 1. Into the first solution (S1), calcium oxalate was synthesized by mixing calcium hydroxide, water and oxalic acid (Ox). Afterwards, TEOS and isopropanol (ISP) were added into the S1 (solution S2) and subjected to magnetic stirring and ultrasonic agitation for 5 and 10 min, respectively. At this stage, the hydrolysis of TEOS started, enhanced by the presence of Ox, which functions as a catalyst [1]. At the same time, solution S3 was prepared, by the addition of PDMS, TEOS and ISP into a separated flask, followed by stirring for 10 min. Finally, the solutions S2 and S3 were mixed at ambient temperature and allowed to stir overnight. Optimization study of raw materials, was determined, which led, after several experiments a product with low viscosity (~ 4 mPa·s) and a crack free xerogel. The final molar ratio of the precursors and solvents TEOS/ISP/H₂O/Ox/CH was equal to 1/10.4/8.01/0.06/0.007.

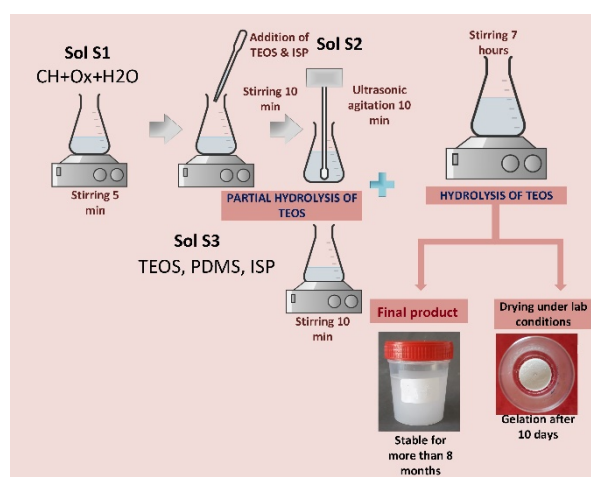


Figure 1. Synthesis route of the nanocomposite.

All chemicals used were not further processed, prior to use. Furthermore, a high molecular weight with polystyrene block copolymer, the commercial dispersant Disperbyk-190 (BYK-Chemie, Wesel) was added during the preparation of the solution, aiming to decrease the surface tension and, consequently, the formation of a monolithic xerogel after drying. Hydrolysis and condensation of TEOS were monitored through FTIR. Furthermore, the stability of the nanocomposite under UV irradiation and humidity was examined through FTIR, after exposing the xerogel in these conditions for 4 days. The analysis was carried out in an FTIR Perkin-Elmer 1000 spectrometer with a resolution of 4 cm^{-1} in the spectral range of $400\text{--}4000\text{ cm}^{-1}$. KBr pellets were used for the homogenization of the examined samples. The formation of CaOx was also examined through TG/DTA. The analysis was performed with a Setaram LabSys Evo 1600 °C thermal analyzer, in static air atmosphere up to 1000 °C at a rate of 10 °C/min . The final solution was cast into cylindrical transparent glass vessels of $\text{Ø}35 \times 38$ mm dimensions. The vessels were properly covered in order to simulate the slow evaporation of the solvent into the pores of the stone substrate. The vessels were exposed to laboratory conditions ($\text{RH} = 60 \pm 5\%$, $T = 20 \pm 2\text{ °C}$).

The xerogel of the nanocomposite was tested through various techniques; the microstructure was observed by scanning and transmission electron microscopy, as well as

via Atomic Force Microscopy (SEM, TEM and AFM respectively). Hardness was measured by a Vickers tester, while surface tension and contact angle were determined using an optical tensiometer. The performance of treated limestones was also examined. Color parameters as well as physical and mechanical properties and microstructure of the samples were checked through colorimetry, digital microscopy, contact angle, water capillarity and ultrasound pulse velocity tests. In particular, the water repellency of treated samples was determined either by measuring Water Contact Angle (WCA) or water absorption by capillarity. The evaluation of the mechanical properties was assessed by measuring Ultrasound Pulse Velocity (UPV). The dynamic modulus of elasticity (Ed_{yn}) according to EN 14,579 (2004), was calculated using the equation:

$$Ed_{yn} = d \times V^2 \quad (1)$$

where: d is the density (kg/m^3) of the sample and V is the ultrasound pulse velocity (m/s).

Concerning the water absorption by capillarity, the water absorption coefficient by capillary (WCA) was estimated by the slope of linear section of the $Qi - \sqrt{ti}$ curve, where Qi is the amount of water absorbed by each sample per unit area (kg/m^2) at time ti (s), calculated by the following equation:

$$Qi = mi - m_0 / A \quad (2)$$

where mi is the mass of the specimen at time ti , in kg; m_0 is the mass of the dry specimen, in kg and A is the area of the sample in contact with water, in m^2 .

3. Results and Discussion

3.1. Characterization of the Nanocomposite

Initially, the properties of the sol nanocomposite and the xerogel of the synthesized product were determined. The viscosity was estimated to be around 4 mPa·s, which enables the penetration of the product into the pores of substrates [9]. Furthermore, the derived xerogel was monolithic and hard as its hardness was measured to 199.3 Vickers. Additionally, the xerogel exhibited 70% volume loss, which is similar with other volume reductions of xerogels referred in the literature [10]. The surface tension of the sol was measured to 30 ± 2 mN/m.

The FTIR spectra of the solution and xerogel are presented in Figure 2. It can be observed that PDMS and TEOS were co-polymerized, whereas the newly formed calcium oxalate has been incorporated into the Si-O-Si network. More particularly, the presence of CaOx can be observed by the bands at 1320 and 1610 cm^{-1} , which are related to the symmetric C-O and asymmetric C=O stretching of CaOx, respectively. It has to be said that around 1610–1650 cm^{-1} there is an overlap between CaOx and the absorbed water bending vibration.

Characteristic bands of PDMS are identified at 2960, 1260 and 800 cm^{-1} . These bands are correlated with the asymmetric C-H stretching bond in CH_3 , the symmetric bending of the CH_3 groups in SiCH_3 and the stretching of Si- CH_3 in PDMS, respectively [11,12]. Moreover, two intense peaks at 1085 and 800 cm^{-1} in spectrum (b), correspond to the Si-O-Si antisymmetric and symmetric stretching vibrations, respectively. The spectrum (a) of the solution is more complicated, due to the overlap of ISP, TEOS and ethanol bands [1]. FTIR spectra of UV- and Humidity-aged xerogel, shown in Figure 2A(e,f) and (c,d) respectively, revealed that the characteristic absorption bands remained unaltered, thus indicating the stability of the xerogel.

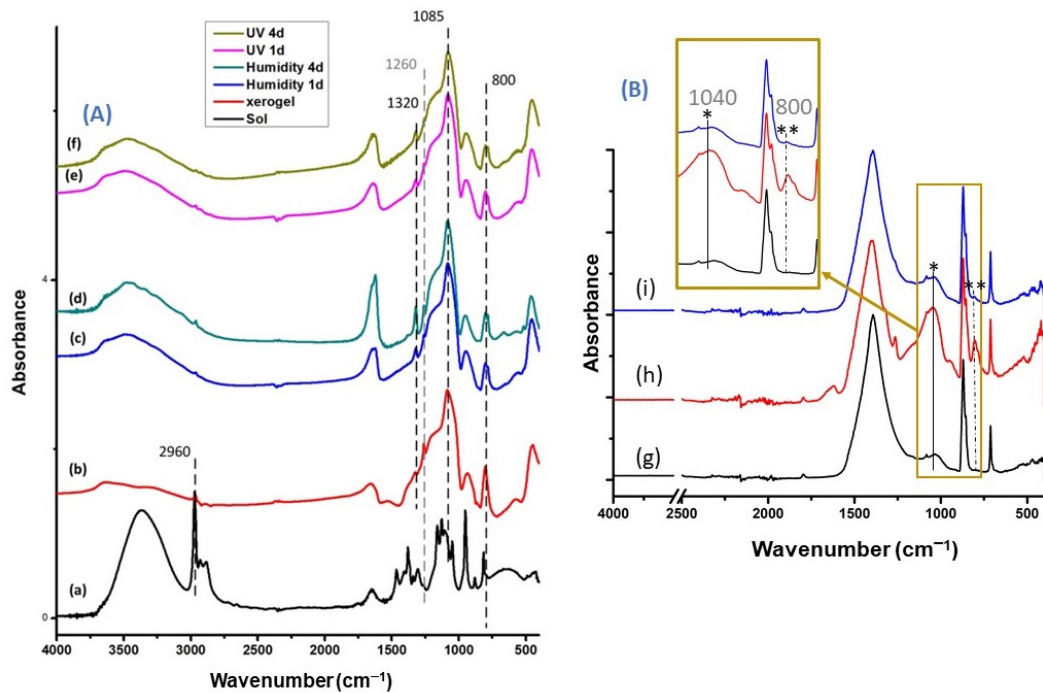


Figure 2. (A) FTIR spectra of: (a) the derived sol, (b) the xerogel, (c) humidity-exposed xerogel for 1 day, (d) humidity-exposed xerogel for 4 days, (e) UV-exposed xerogel for 1 day and (f) UV-exposed xerogel for 4 days (B) spectra of: (g) untreated surface, (h) treated surface and (i) powder of treated matrix in a depth of 2 cm from the surface.

Furthermore, Figure 3A displays the TG/DTA curves of the xerogel. According to this analysis, two endothermic peaks are observed due to the thermal decomposition of di-hydrated CaOx at 138 and 220 °C [13]. The corresponding mass losses during these 2 endothermic reactions at 138 and 220 °C are 12.9% and 30.5%, respectively.

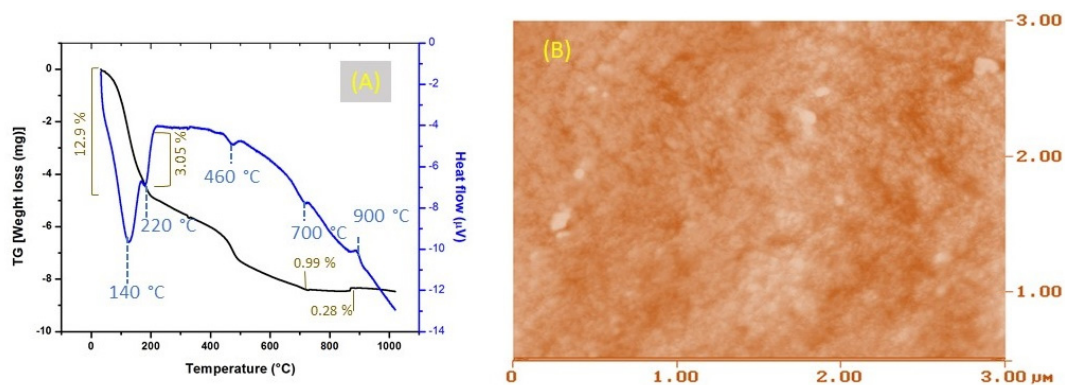


Figure 3. (A) TG/DTA curves of the xerogel (B) AFM image of xerogel.

TEM images, presented in Figure 4A, showed that the nanocomposite has an aggregated form, fact that could be attributed to the polymeric chain alteration, derived from the CaOx and PDMS incorporation via electrostatic interactions and hydrogen bonding. In particular, TEM images demonstrated two phases; the first covered a large area of the nanocomposite, consisted of amorphous SiO₂, while the second one included a semi-crystalline structure of the product in nanoscale. The semi-crystallinity of the product was also proved by the characteristic pattern, evidenced at Figure 4A(e), captured with high magnification. In Figure 4B the SEM micrographs of xerogel are presented. The surface of xerogel is characterized as rough and crack-free. The roughness of surface is attributed to TEOS and PDMS copolymerization process. EDS analysis, presented in Figure 4B(b), showed that, xerogel was mainly silicon based. The roughness of the xerogel surface was

also observed through AFM, as shown in Figure 3B, which was highly heterogeneous with patchy areas. The arithmetic mean of the roughness (Ra) and the square root (Rq) were approximately 3.369 and 4.342 nm, respectively. This finding was remarkable, as the roughness of traditional consolidants has been lower [14], giving rise to the hydrophobicity of the product.

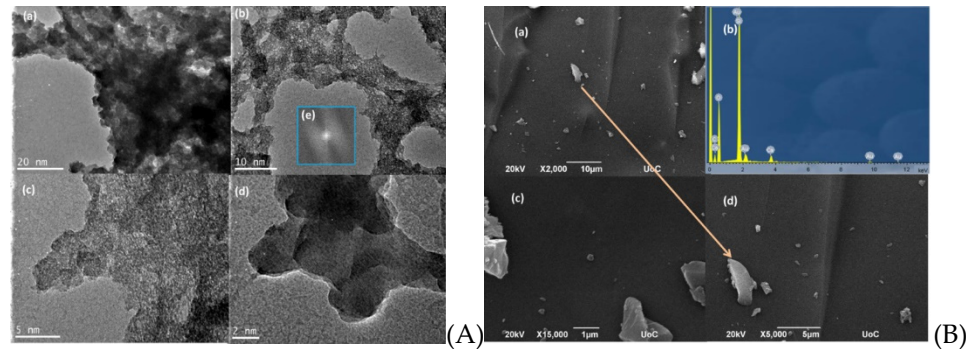


Figure 4. (A) TEM images of different magnification (a–d) and (e) indication of crystalline structure, (B) SEM images of xerogel and EDS analysis: (a,c) Images captured from random areas of the consolidant, (d) magnified image of the area selected at (c) and (b) EDS results.

3.2. Evaluation of Consolidant Performance on Limestones

The impregnation treatment was applied by brushing on 3 groups of alfas stones of different shape, consisting of 5 specimens each, as illustrated in Figure 5. The 3 groups of stones of the same composition have been quarried at the same time, and shaped differently, fact that may affect UPV measurements. The uptake and dry matter of the consolidant was $36.47 \pm 8.06 \times 10^{-3}$ and $10.51 \pm 1.73 \times 10^{-3}$ g/cm², respectively. The penetration depth was found at least 2 cm from the surface as indicated by the absorptions of Si-O-Si bonds, 1040 and 800 cm⁻¹, in Figure 2B(h,i). Digital microscopy images illustrated in Figure 6A, showed that the treated surface exhibited a crack-free appearance with homogeneous distribution of the product. The color alterations were also evaluated by determining the L*, a* and b* parameters using a chromatometer.

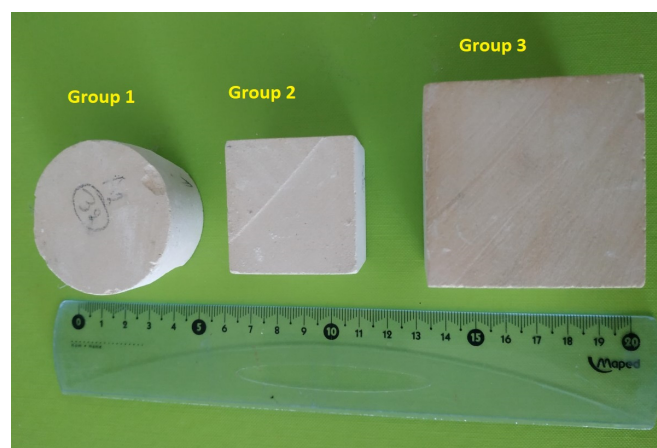


Figure 5. Different samples from each group of treatment.

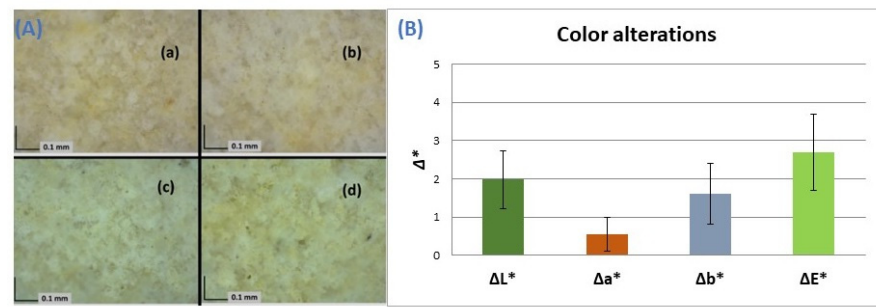


Figure 6. (A) Images from digital microscope (a,b) treated surfaces, (c,d) untreated surfaces. (B) Color difference ΔE^* (\pm stdv) induced after the treatment application, for all the investigated sample groups.

The ΔE^* parameter calculated by the Equation (3), refers to the colour alteration of the surface.

$$\Delta E = \sqrt{\Delta L^2 + \Delta a^2 + \Delta b^2} \quad (3)$$

ΔE^* parameter less than 3 is a perceptible difference from the human eye, whereas ΔE^* up to 5 is an acceptable value [15,16] concerning monochrome surfaces as in our case with alfas limestones. The determination of ΔE^* parameter presented in Figure 6B, revealed that the measured color changes range within acceptable limits.

Waterproofing was also significantly improved, as revealed by the WCA measurements and capillary absorption test. A hydrophobic layer was formed after treatment was applied, WCA measurements were more than 90° . However, on untreated surfaces the WCA couldn't be measured, as the water droplet was absorbed immediately. In addition, the water capillary coefficient (WCC), calculated by the slope of the linear section of the curves of water capillary absorption illustrated in Figure 7 has decreased by $94.4 \pm 2.3\%$, proving that the synthesized nanocomposite effectively protects against the action of water. It was observed that before treatment, the 3rd group of stones absorbed larger amount of water at the same rate comparing to the other two groups. This could be explained by the different height of those specimens that allowed the capillary rise to be accomplished in different saturation time and amount of total absorbed water. Evidence of this statement was the similar trend observed in capillary water absorption after treatment.

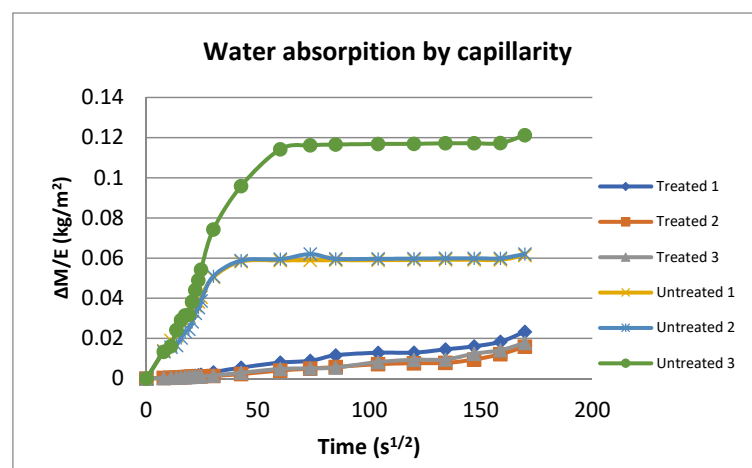


Figure 7. Water absorption by capillarity curves of treated and untreated groups of samples.

The ultrasound pulse velocity (UPV) of untreated and treated samples was measured in order to evaluate improvement in the mechanical behavior. The UPV was measured before the treatment of the surface and after 2 weeks and 1 month of the surface consolidation. The dynamic modulus of elasticity (E_{dyn}) shown in Figure 8, exhibited an increasing tendency after 2 weeks to 1 month of treatment.

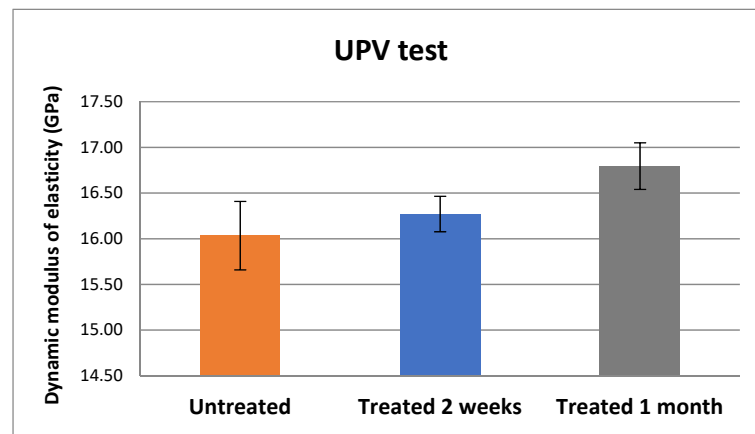


Figure 8. Dynamic modulus of elasticity of untreated and treated stones measured 2 weeks and 1 month after curing.

4. Conclusions

A novel consolidant product was synthesized in a simplified procedure, incorporating to TEOS, PDMS and nano calcium oxalate. This product exhibits high affinity with carbonate stones, due to the presence of calcium oxalate. The aforementioned nanocomposite is stable under UV and moisture exposure. Furthermore, the derived product was tested on Cretan limestones, where it penetrated at least 2 cm into the substrate improving the mechanical properties, such as dynamic modulus of elasticity. Water repellency of the treated samples was significantly increased as indicated from WCA and water absorption by capillarity test. In treated samples WCC capillary coefficients decreased by 94.4% and WCA was more than 90°. The treated surfaces showed a crack-free appearance and the color parameters conform with the criteria imposed by the international standards for stone treatment. Based on the results presented above, it can be confirmed that the synthesized product is a powerful consolidant with protective features for stone conservation.

Author Contributions: Conceptualization, P.-N.M.; methodology, P.-N.M.; software, P.-N.M.; validation, P.-N.M., K.K. and D.S.; formal analysis, K.K.; investigation, K.K. and D.S.; resources, P.-N.M.; data curation, P.-N.M.; writing—original draft preparation, K.K.; writing—review and editing, P.-N.M.; visualization, P.-N.M.; supervision, P.-N.M.; project administration, P.-N.M.; funding acquisition, P.-N.M. All authors have read and agreed to the published version of the manuscript.

Funding: This work has been supported by the InnovaConcrete project funded by the European program Horizon 2020 (GA No. 760858).

Institutional Review Board Statement: Not applicable.

Informed Consent Statement: Not applicable.

Data Availability Statement: Data available on request from the authors.

Conflicts of Interest: The authors declare no conflict of interest.

References

- Verganelaki, A.; Kapridaki, C.; Maravelaki-Kalaitzak, P. Modified Tetraethoxysilane with Nanocalcium Oxalate in One-Pot. *Ind. Eng. Chem. Res.* **2015**, *54*, 7195–7206. [[CrossRef](#)]
- Sierra-Fernandez, A.; Gomez-Villalba, L.S.; Rabanal, M.E.; Fort, R. New nanomaterials for applications in conservation and restoration. *Mater. Construcción* **2017**, *67*, 325.
- Gemelli, G.M.C.; Zarzuela, R.; Fernandez, F.; Mosquera, M.J. Compatibility, effectiveness and susceptibility to degradation of alkoxy-silane-based consolidation treatments on a carbonate stone. *J. Build. Eng.* **2021**, *42*, 102840. [[CrossRef](#)]
- Maravelaki-Kalaitzaki, P.; Kallithrakas-Kontos, N.; Korakaki, D.; Agioutantis, Z.; Maurigiannakis, S. Evaluation of Silicon-Based Strengthening Agents on Porous Limestones. *Prog. Org. Coat.* **2006**, *57*, 140–148. [[CrossRef](#)]
- Ion, R.M.; Teodorescu, S.; Știrbescu, R.M.; Bucurică, I.A.; Dulamă, I.D.; Ion, M.L. Calcium Oxalate on Limestone Surface of Heritage Buildings. *Key Eng. Mater.* **2017**, *750*, 129–134. [[CrossRef](#)]

6. Rampazzi, L. Calcium oxalate films on works of art: A review. *J. Cult. Herit.* **2019**, *40*, 195–214. [[CrossRef](#)]
7. Nomikos, P.; Kaklis, K.; Agioutantis, Z.; Mavrigiannakis, S. Investigation of the size effect and the fracture process on the uniaxial compressive strength of the banded Alfas porous stone. *Procedia Struct. Integr.* **2020**, *26*, 285–292. [[CrossRef](#)]
8. Verganelaki, A.; Maravelaki, N.; Kilikoglou, V.; Karatasios, I.; Arampatzis, I.; Siamos, K. Characterization of a Newly Synthesized Calcium Oxalate-Silica Nanocomposite and Evaluation of Its Consolidation Effect on Limestones. In *Built Heritage. Monitoring Conservation Management*; Boriani, M., Guidi, G., Toniolo, L., Eds.; Springer: Berlin/Heidelberg, Germany, 2015; pp. 391–402.
9. Franzoni, E.; Graziani, G.; Sassoni, E.; Bacilieri, G.; Griffa, M.; Lura, P. Solvent-based 668 ethyl silicate for stone consolidation: Influence of the application technique on penetration depth, 669 efficacy and pore occlusion. *Mater. Struct.* **2014**, *48*, 3503–3515. [[CrossRef](#)]
10. Facio, D.S.; Carrascosa, L.A.M.; Mosquera, M.J. Producing lasting amphiphobic building surfaces with self-cleaning properties. *Nanotechnology* **2017**, *28*, 265601. [[CrossRef](#)] [[PubMed](#)]
11. Kapridaki, C.; Maravelaki-Kalaitzak, P. TiO₂-SiO₂-PDMS nano-composite hydrophobic coating with self-cleaning properties for marble protection. *Prog. Org. Coat.* **2013**, *76*, 400–410. [[CrossRef](#)]
12. Kapridaki, C.; Verganelaki, A.; Dimitriadou, P.; Maravelaki-Kalaitzaki, P. Conservation of Monuments by a Three-Layered Compatible Treatment of TEOS-Nano-Calcium Oxalate Consolidant and TEOS-PDMS-TiO₂ Hydrophobic/Photoactive Hybrid Nanomaterials. *Materials* **2018**, *11*, 684. [[CrossRef](#)] [[PubMed](#)]
13. Frost, R.L.; Weier, M.L. Thermal Treatment of Whewellite-A Thermal Analysis and Raman Spectroscopic Study. *Thermochim. Acta* **2004**, *409*, 79–85. [[CrossRef](#)]
14. Petronella, F.; Pagliarulo, A.; Truppi, A.; Lettieri, M.; Masieri, M.; Calia, A. TiO₂ Nanocrystal Based Coatings for the Protection of Architectural Stone: The Effect of Solvents in the Spray-Coating Application for a Self-Cleaning Surfaces. *Coatings* **2018**, *8*, 356. [[CrossRef](#)]
15. De Rosario, I.; Felhaddad Pan, A.; Benavides, R.; Rivas, T.; Mosquera, M.J. Effectiveness of a novel consolidant on granite: Laboratory and in situ results. *Construction* **2015**, *76*, 140–149. [[CrossRef](#)]
16. Ksinopoulou, E.; Bakolas, A.; Moropoulou, A. Modifying Si-based consolidants through the addition of colloidal nano-particles. *Appl. Phys. A* **2016**, *122*, 267. [[CrossRef](#)]